Anomalous Dislocation Multiplication in FCC Metals

Maurice de Koning, Wei Cai, and Vasily V. Bulatov
Lawrence Livermore National Laboratory, P.O. Box 808, L-371, Livermore, California 94550, USA
(Received 11 February 2003; published 8 July 2003)

Direct atomistic simulations of dislocation multiplication in fcc aluminum reveal an unexpected mechanism, in which a Frank-Read source emits dislocations with Burgers vectors different from that of the source itself. The mechanism is traced to a spontaneous nucleation of partial dislocation loops within the stacking fault. Understanding and a quantitative description of this unusual process are achieved through the development of a continuum model for dislocation nucleation based on the coarse-grained dislocation dynamics approach and a minimal amount of atomistic input.

DOI: 10.1103/PhysRevLett.91.025503 PACS numbers: 61.72.Lk, 02.70.Ns, 62.20.Fe

Mechanical strength of crystalline solids is controlled mainly by the dynamics of dislocations—line defects that carry plastic deformation through the crystal lattice. In particular, the malleability of metals and alloys is associated with the well-recognized ability of dislocations to rapidly multiply under stress. A generally accepted model for such multiplication is the Frank-Read (FR) source [1], i.e., a dislocation segment pinned between two fixed points. As shown in Fig. 1, when the stress exceeds a critical value, the bowing out of the dislocation segment becomes unstable, leading to the regenerative emission of dislocation loops, each carrying the same Burgers vector as that of the original pinned segment. This sequence is viewed as the classical dislocation multiplication mechanism: FR sources are routinely observed in *in situ* TEM experiments [2] and the calculation of their activation stresses is a standard exercise in the continuum linear-elastic theory of dislocations [3]. An aspect that has not been examined so far, however, concerns possible effects of the nonlinear dislocation core on this process.

In this Letter, we present the first direct atomistic study of FR source operation in fcc aluminum that reveals a surprising variation to the classical concept of dislocation multiplication. In particular, we observe that, depending on the applied stress, a source with Burgers vector $\mathbf{b}_1$ may emit dislocation loops with a *different* Burgers vector $\mathbf{b}_2$. This anomalous mechanism is a manifestation of a strong nonlinear core effect in fcc metals: it results from the nucleation of a partial dislocation loop inside the intrinsic stacking-fault (ISF) area. To obtain further insight into this peculiar behavior, we develop a dislocation-dynamics-based continuum model whose predictions are in good agreement with the atomistic results. The model enables us to examine the physical origin of the anomalous multiplication mode, and predicts that it can operate in fcc metals and alloys with relatively high ISF and low unstable stacking-fault (USF) energies [4–7]. Moreover, the study presents a semianalytical theory of dislocation nucleation in spatially heterogeneous stress fields that should be applicable in a much wider context of related phenomena.

For our atomistic simulations we use a computational cell containing 1.15×10^5 atoms with the edges $40[\bar{1}10]$, $8[111]$, and $15[11\bar{2}]$, replicated periodically in all three directions. The FR source is constructed as a rectangular-shaped dislocation loop inside an otherwise perfect fcc crystal. To create the loop, a $4[111] \times 5[11\bar{2}]$ plate of atoms is removed from a $(\bar{1}10)$ atomic plane. The atomic configuration is then relaxed through conjugate-gradient energy minimization under the zero-stress boundary conditions [8] using the Ercolessi-Adams (EA) potential for aluminum [9]. The result, shown in Fig. 2(a), is a prismatic dislocation loop consisting of two edge dislocation dipoles with Burgers vector $\mathbf{b}_1 = \mathbf{AB}$ [in standard Thompson tetrahedron notation [3]; see Fig. 2(b)]. Starting from this configuration, we then investigate the behavior of the source as a function of magnitude and orientation of stress applied in the (111) glide plane.

Figures 2(c) and 2(d) show atomistic simulation snapshots illustrating, respectively, normal and anomalous FR operation on one of the two glide planes of the loop. Figure 2(c) presents a case for which the shear stress is applied parallel to $\mathbf{b}_1$, inflicting equal forces on the leading (outer) and the trailing (inner) partials, with Burgers vectors $\mathbf{b}_{p_1} = \mathbf{A\delta}$ and $\mathbf{b}_{p_2} = \mathbf{\delta B}$, respectively, resulting in the emission of dislocation loops with Burgers vector $\mathbf{b}_1$, according to the normal FR mechanism (Fig. 1).

The scenario shown in Fig. 2(d) is remarkably different. In this simulation the stress is applied along the $[0\bar{1}1]$ or **CA** direction, i.e., perpendicular to the Burgers vector

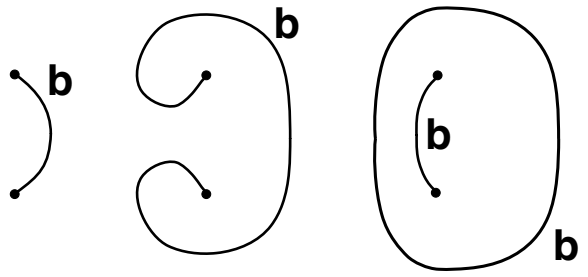

FIG. 1. Schematics of the Frank-Read (FR) source mechanism for dislocation multiplication (see text).

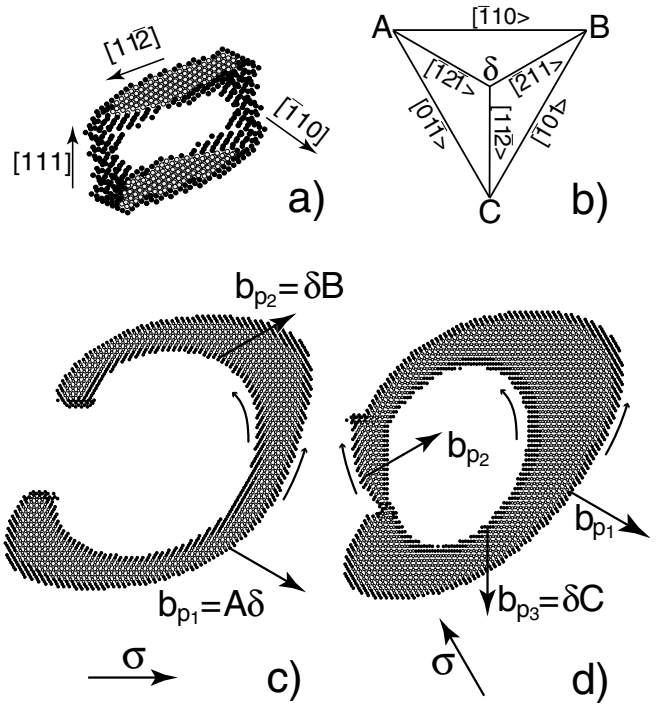

FIG. 2. FR source operation in Ercolessi-Adams aluminum. Only atoms in the dislocation cores and ISF areas are shown. Orientation of applied stress σ and dislocation line senses (curved arrows) are also indicated. (a) Relaxed prismatic loop configuration at zero stress. Two mobile (glissile) segments lie along the $[11\bar{2}]$ direction and dissociate into pairs of Shockley partial dislocations (partials) on the (111) planes, while two compact and relatively immobile (sessile) segments lie along the [111] directions. In this way, the corners of the rectangular loop serve as pinning points for the glissile segments, creating two FR sources. (b) The (111) face of the Thompson tetrahedron (viewed from outside) [3]. (c) Conventional multiplication. (d) Anomalous multiplication.

of the trailing partial. Here, only the leading partial moves, extending the ISF area until, at some point, a small dislocation loop nucleates inside the ISF, clearing the fault and restoring the normal fcc coordination across its area. The Burgers vector of this loop is that of the third partial in the (111) glide plane [3], $\mathbf{b}_{p_3} = \boldsymbol{\delta}\mathbf{C}$. After nucleation, the loop grows in size, clearing the ISF until its leading segment catches up with the leading partial $\mathbf{b}_{p_1}$. Both segments then continue to expand together, giving rise to the emission of a dislocation loop with Burgers vector $\mathbf{b}_2 = \mathbf{b}_{p_1} + \mathbf{b}_{p_3} = \mathbf{AC}$, which is *different* from that of the original source dislocation, $\mathbf{b}_1$. The remaining portion of the nucleated dislocation loop joins the trailing partial $\mathbf{b}_{p_2}$, forming a straight dislocation segment between the pinning points, with Burgers vector $\mathbf{b}_3 = \mathbf{b}_{p_2} - \mathbf{b}_{p_3} = \mathbf{CB}$. As a result, the total Burgers vector is conserved in these reactions, $\mathbf{b}_1 = \mathbf{b}_2 + \mathbf{b}_3$. Moreover, the mechanism is regenerative: after a loop pinches off, its remnant segment with Burgers vector $\mathbf{b}_2$ recombines with the pinned dislocation $\mathbf{b}_3$, reestablishing the initial FR source configuration with Burgers vector $\mathbf{b}_1$.

The minimum (critical) stress required to produce a full dislocation loop was computed for various stress orientations in the (111) glide plane. The results are shown in Fig. 3, in which the stress magnitude (radius) is plotted as a function of the stress direction angle θ, measured counterclockwise with respect to $\mathbf{b}_1$. As a reference, the ideal shear resistance of a dislocation-free crystal was also computed (circles). Consistent with the notion that the latter provides an upper limit, the critical stress values for the FR source (diamonds) fall entirely within the ideal-resistance envelope. The stress reduction is most evident in the angular range between approximately $\theta = -30°$ and 210°, where FR source operation is responsible for yielding. Only in a narrower range, between approximately $\theta = 60°$ and 120°, does the source operate anomalously [as in Fig. 2(d)]. In the range between $\theta = 240°$ and 300°, the FR source itself is not activated, resulting in a critical stress very close to the ideal resistance.

To clarify the physical origin of the observed anomalous behavior and enable a quantitative prediction of its activity, we contrast the atomistic results with a continuum model. For this purpose, the atomistic results are compared to dislocation dynamics (DD) predictions obtained for the same FR source using identical boundary conditions. We use a nodal-representation DD model [10] in which partial dislocations and the associated ISF areas are resolved explicitly [11]. For simplicity we use the isotropic elasticity solution for the interaction energy between dislocations, with the elasticity parameters and the ISF energy γ_I matched to the EA potential values. For the only parameter extrinsic to the continuum theory of dislocations, the core radius r_c (see, e.g., Ref. [3], pp. 231–232), a value of $r_c = 0.173b_p$ ($b_p = |\mathbf{b}_{p_i}|$, $i = 1, 2, 3$) is adopted to reproduce the atomistic activation stress computed for the orientation $\theta = 0°$, where the source

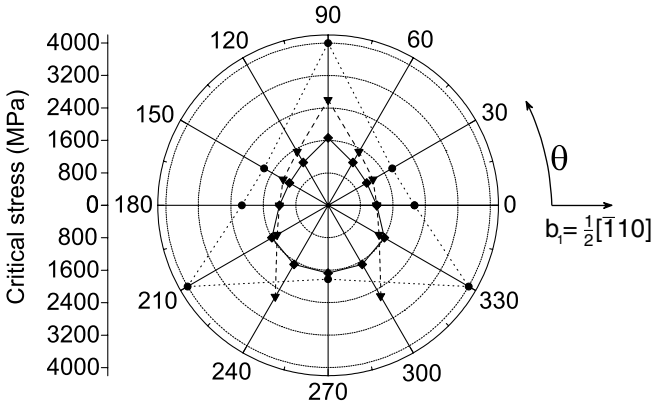

FIG. 3. Ideal shear resistance stress (circles) and FR source activation stress (diamonds) as a function of stress orientation in (111) plane. Triangles show FR activation results obtained from DD model.

operates normally. The resulting DD activation stress envelope is shown as the triangles in Fig. 3. For the orientations in which the atomistic FR source is seen to operate normally, i.e., from $\theta = -30°$ to 30°, the atomistic and the DD predictions agree quite well. However, in the angular range where anomalous multiplication is observed, i.e., for $\theta = 60°$, $\theta = 90°$, and $\theta = 120°$, the results are clearly different. This discrepancy is not at all surprising, given that the DD model does not allow for loop nucleation and needs to be *informed,* through a nucleation criterion, about conditions under which the loop formation becomes possible.

To better understand this nucleation process, we first examine the simpler case of an infinitely long edge dislocation with Burgers vector $\mathbf{b}_1$ dissociated into two parallel partials $\mathbf{b}_1 = \mathbf{b}_{p_1} + \mathbf{b}_{p_2}$. The equilibrium width of the ISF is determined by the balance between the elastic repulsion among the partials, the ISF energy, and the external stress [3]. Among the six components of the general stress tensor, the splitting width is affected only by the Escaig stress, i.e., the component perpendicular to the total Burgers vector $\mathbf{b}_1$ in the glide plane (111). When this component approaches a critical value of $\sigma_{\mathrm{SF}} = 2\gamma_I/b_p$, the dissociation width should become infinite. For the EA model, this happens at $\sigma_{\mathrm{SF}} = 1.284$ GPa. However, direct atomistic calculations show [12] that well below that value, at $\sigma_E^* = 0.93 \pm 0.05$ GPa, a dipole of Shockley partials with Burgers vector $\mathbf{b}_{p_3}$ spontaneously nucleates inside the ISF, splitting the initial dislocation into two others according to the same reaction seen in the anomalous multiplication scenario, $\mathbf{b}_1 \rightarrow \mathbf{b}_2 + \mathbf{b}_3$.

This process is analyzed here within a simple linear-elastic framework augmented by a nonlinear atomistic term, in the form of a generalized stacking-fault (GSF) energy function [4–7], in the spirit of the Peierls-Nabarro model [13] and an earlier treatment by Saada [14]. The model involves only three variables, as shown in Fig. 4(a): the separation L between the two initial partials $\mathbf{b}_{p_1}$ and $\mathbf{b}_{p_2}$, the width R of the incipient dipole, and the continuous fractional Burgers vector of the dipole $\mathbf{b}_d = \delta\,\mathbf{b}_{p_3}$ with $\delta \in [0, 1]$. As δ changes from 0 to 1, the area swept by the incipient dipole transforms from an ISF to perfect crystal. The associated energy change, per unit area of the fault, is described by the GSF function $\gamma_{\mathrm{GSF}}(\delta)$ along the $[11\bar{2}]$ direction, plotted in Fig. 4(b). Assuming an Escaig stress σ_E is applied, the energy per unit length of the dislocation assembly $(\mathbf{b}_{p_2}, -\delta\mathbf{b}_{p_3}, \delta\mathbf{b}_{p_3}, \mathbf{b}_{p_1})$ is then given by

$$W(L, R, \delta; \sigma_E) = -\frac{1}{8\pi(1-\nu)}\mu b_p^2(2+\nu)\ln\left(\frac{L}{\alpha b_p}\right) + \frac{1}{2\pi}\mu\delta^2 b_p^2 \ln\left(\frac{R}{\alpha\delta b_p}\right) + \frac{1}{2\pi}\mu\delta b_p^2 \ln\left(\frac{L+R}{L-R}\right) - \sigma_E\left(\frac{1}{2}b_p L + \delta b_p R\right) + \gamma_I(L-R) + \gamma_{\mathrm{GSF}}(\delta)R, \quad (1)$$

where the first term is the energy of elastic interaction between the two initial partials, the second describes the self-energy of the incipient dipole, and the third is the interaction energy of the incipient dipole and both preexisting partials. In the dipole self-energy term we assume that the core radius of the incipient dislocations is proportional to their Burgers vector by the same factor $\alpha = 0.173$ used earlier. The last three terms represent the work done by the external stress and the fault energy. Within this model, dipole nucleation inside the ISF is viewed as a loss of stability of the initial state ($\delta = 0, R = 0$) towards $R \rightarrow \infty$ and $\delta \rightarrow 1$, with increasing σ_E. At a stress just below the critical value σ_E^*, W still contains a metastable state ($\delta \sim 0.1, R \sim 30b_p$) in which the ISF remains essentially intact. Beyond σ_E^* this minimum becomes unstable, and a fully developed dislocation dipole forms spontaneously. This condition occurs at $\sigma_E^* = 1.00 \pm 0.02$ GPa, in good agreement with the atomistic prediction reported above.

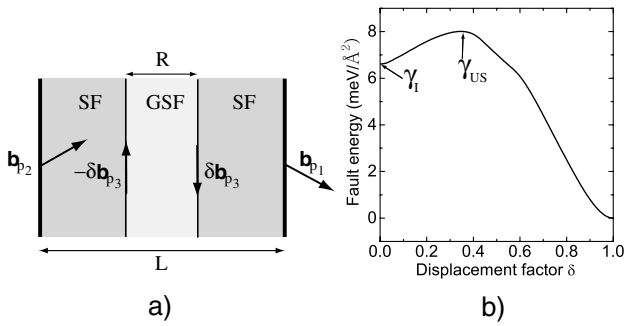

FIG. 4. (a) Schematic representation of variables in model describing straight partial dislocation dipole nucleation. (b) Generalized stacking-fault function $\gamma_{\mathrm{GSF}}(\delta)$ for EA potential. Intrinsic and unstable stacking-fault energies are marked γ_I and γ_{us}, respectively.

Returning to the case shown in Fig. 2(c), we now consider the energetics of loop nucleation in a similar setting. To simplify the calculations, we assume that the incipient loop is a circle of radius R centered at the point of maximum Escaig stress component inside the ISF, and that the original partials remain fixed during its formation. The loop energy then becomes

$$W(R, \delta; \sigma_E) = \mu\delta^2 b_p^2 R\frac{2-\nu}{4(1-\nu)}\left[\ln\left(\frac{R}{\alpha\delta b_p}\right) - 2\right] + \pi R^2\gamma_{\mathrm{GSF}}(\delta) - 2\pi\delta b_p\left[\int_0^R \tau_{\mathrm{int}}(r)r\,dr + \frac{\sigma_E R^2}{2}\right], \quad (2)$$

where the three terms represent the self-energy of the incipient loop, the fault energy, and the work done by the total stress, respectively. The latter includes both the applied stress σ_E and the internal stress field due to

the initial partials $\tau_{\text{int}}(r)$, which is assumed to be radially symmetric about the center of the incipient loop. The function $\tau_{\text{int}}(r)$ is computed using a DD model that makes no account of the incipient loop. This is accomplished by finding an equilibrium position of the preexisting partials under the applied stress σ_E, followed by the calculation of internal stress they produce. As before, the nucleation stress is determined by identifying the onset of an instability of Eq. (2) as σ_E is increased [12].

For the case of $\theta = 90°$ in Fig. 3, the above analysis reveals that at $\sigma_E^* = 1.72 \pm 0.05$ GPa, loop formation and subsequent anomalous source activation become energetically favorable. This lowers significantly the previous DD prediction of $\sigma_E^* \sim 2.6$ GPa and brings it in excellent agreement with the atomistic result $\sigma_E^* = 1.66 \pm 0.02$ GPa shown in Fig. 3. Remarkably, for the $\theta = 60°$ and 120° cases, the nucleation model predicts that loop formation is not a necessary stage of source activation, and occurs only *after* the source has been activated, again in agreement with the atomistic observation.

Given the success of the continuum models (1) and (2) in reproducing the atomistic results, we examined which parameters are most relevant in defining a material's propensity to anomalous multiplication. We find that this tendency increases with a decreasing ratio between the maximum slope of the GSF energy function along the rise between the ISF and USF configurations [see Fig. 4(b)] and γ_I, as the nucleation stress σ_E^* becomes smaller than $\sigma_{\text{SF}} = 2\gamma_I/b_p$ [12]. However, high stress in itself is not sufficient: to occur, loop nucleation also requires *room;* i.e., the stress should be sufficiently high across a sufficiently large area of the nucleation plane.

The quantitative match between the atomistic simulations and the continuum models also allows us to replace the EA-based GSF function and probe the activity of the anomalous multiplication mechanism using a more accurate electronic-structure-based description. This analysis confirms that anomalous source operation is expected to be active in fcc Al [5] as well as in Pt [7]. However, even for these materials, the activation stress is rather high, of the order of 1 GPa. This implies that, although less likely to play a role under low-stress deformation conditions, the anomalous multiplication mechanism is predicted to become important in shock loading and/or nanoindentation experiments during which such high stress levels are routinely reached [15]. While explicit experimental verification remains necessary, anomalous source operation has indeed been recently observed in large-scale molecular dynamics simulations of deformation of Al nanocrystals [16], using the same EA potential. The same simulations revealed yet another closely related behavior [17]: dislocations were seen to collide with extended ISF areas, resulting in their perforation by means of the same partial dipole nucleation mechanism discussed here.

In summary, we have studied FR source operation in fcc Al using a combination of atomistic and DD simulation approaches. We report that a source can, under certain conditions, emit dislocation loops with Burgers vectors different from that of the source itself. This anomalous mechanism is driven by the nucleation of a partial dislocation loop inside the ISF. It is expected to be important under high strain rate deformation conditions and is accurately described by a simple continuum model that uses only a minimal amount of atomistic input, the GSF function. The latter is now routinely computed using the most accurate *ab initio* methods, making it possible to examine a number of related problems, including dislocation nucleation in nanoindentation [13,18] and the competition between dislocation and twinning modes of deformation [19].

This work was performed under the auspices of the U.S. Department of Energy by the University of California, Lawrence Livermore National Laboratory under Contract No. W-7405-Eng-48. M. K. and V. V. B. acknowledge support from the ASCI Dynamics of Metals Program and the Computational Materials Science Network. W. C. is supported by the University Relationship Program at LLNL. We thank Tomas Diaz de la Rubia and Elaine Chandler for their continued interest and support.

[1] F. C. Frank and W. T. Read, in *Symposium on Plastic Deformation of Crystalline Solids* (Carnegie Institute of Technology, Pittsburgh, 1950), p. 44.
[2] J. Rabier, F. Sandiumenge, J. Plain, A. Proult, and I. Stretton, Philos. Mag. Lett. **82**, 419 (2002).
[3] J. P. Hirth and J. Lothe, *Theory of Dislocations* (Krieger Publishing Company, Malabar, FL, 1992), 2nd ed.
[4] V. Vitek, Philos. Mag. **18**, 773 (1968).
[5] G. Lu, N. Kioussis, V. V. Bulatov, and E. Kaxiras, Phys. Rev. B **62**, 3099 (2000).
[6] J. A. Zimmerman, H. Gao, and F. F. Abraham, Model. Simul. Mater. Sci. Eng. **8**, 103 (2000).
[7] M. J. Mehl, D. A. Papaconstantopoulos, N. Kioussis, and M. Herbranson, Phys. Rev. B **61**, 4894 (2000).
[8] M. Parrinello and R. Rahman, J. Appl. Phys. **52**, 7182 (1981).
[9] F. Ercolessi and J. B. Adams, Europhys. Lett. **26**, 583 (1994).
[10] K. W. Schwartz, J. Appl. Phys. **85**, 108 (1999).
[11] V. B. Shenoy, R. V. Kukta, and R. Phillips, Phys. Rev. Lett. **84**, 1491 (2000).
[12] M. de Koning, W. Cai, and V. V. Bulatov (to be published).
[13] V. B. Shenoy, R. Phillips, and E. B. Tadmor, J. Mech. Phys. Solids **48**, 649 (2000).
[14] G. Saada, Acta Metall. **10**, 551 (1962).
[15] A. Loveridge-Smith *et al.*, Phys. Rev. Lett. **86**, 2349 (2001).
[16] V. Yamakov, D. Wolf, S. R. Phillpot, A. K. Mukherjee, and H. Gleiter, Nature Materials **1**, 45 (2002).
[17] V. Yamakov, D. Wolf, S. R. Phillpot, and H. Gleiter, Acta Mater. (to be published).
[18] J. Li, K. J. van Vliet, T. Zhu, S. Yip, and S. Suresh, Nature (London) **418**, 307 (2002).
[19] S. Hai and E. B. Tadmor, Acta Mater. **51**, 117 (2003).